



Archived at the Flinders Academic Commons:

<http://dspace.flinders.edu.au/dspace/>

The following article appeared as:

Kato, H., Asahina, T., Masui, H., Hoshino, M., Tanaka, H., Cho, H., Ingolfsson, O., Blanco, F., Garcia, G., Buckman, S.J. and Brunger, M.J., 2010. Substitution effects in elastic electron collisions with CH_3X ($\text{X} = \text{F}, \text{Cl}, \text{Br}, \text{I}$) molecules. *Journal of Chemical Physics*, 132, 074309.

and may be found at:

http://jcp.aip.org/resource/1/jcpsa6/v132/i7/p074309_s1

DOI: <http://dx.doi.org/10.1063/1.3319761>

Copyright (2010) American Institute of Physics. This article may be downloaded for personal use only. Any other use requires prior permission of the authors and the American Institute of Physics.

Substitution effects in elastic electron collisions with CH₃X (X = F, Cl, Br, I) molecules

H. Kato, T. Asahina, H. Masui, M. Hoshino, H. Tanaka et al.

Citation: *J. Chem. Phys.* **132**, 074309 (2010); doi: 10.1063/1.3319761

View online: <http://dx.doi.org/10.1063/1.3319761>

View Table of Contents: <http://jcp.aip.org/resource/1/JCPSA6/v132/i7>

Published by the [American Institute of Physics](#).

Additional information on *J. Chem. Phys.*

Journal Homepage: <http://jcp.aip.org/>

Journal Information: http://jcp.aip.org/about/about_the_journal

Top downloads: http://jcp.aip.org/features/most_downloaded

Information for Authors: <http://jcp.aip.org/authors>

ADVERTISEMENT



Goodfellow
metals • ceramics • polymers • composites
70,000 products
450 different materials
small quantities fast

www.goodfellowusa.com

Substitution effects in elastic electron collisions with CH₃X (X=F, Cl, Br, I) molecules

H. Kato,¹ T. Asahina,¹ H. Masui,¹ M. Hoshino,¹ H. Tanaka,¹ H. Cho,² O. Ingólfsson,³ F. Blanco,⁴ G. Garcia,⁵ S. J. Buckman,⁶ and M. J. Brunger⁷

¹Department of Physics, Sophia University, Tokyo 102-8554, Japan

²Department of Physics, Chungnam National University, Daejeon 305-764, South Korea

³Department of Chemistry, Science Institute, University of Iceland, Reykjavík 107, Iceland

⁴Departamento de Física Atómica, Molecular y Nuclear, Universidad Complutense de Madrid, Madrid 28040, Spain

⁵Instituto de Física Fundamental, Consejo Superior de Investigaciones Científicas, Madrid 28006, Spain

⁶ARC Centre for Antimatter-Matter Studies, Australian National University, Canberra, ACT 0200, Australia

⁷ARC Centre for Antimatter-Matter Studies, Flinders University, G.P.O. Box 2100, Adelaide, South Australia 5001, Australia

(Received 23 November 2009; accepted 26 January 2010; published online 19 February 2010)

We report absolute elastic differential, integral, and momentum transfer cross sections for electron interactions with the series of molecules CH₃X (X=F, Cl, Br, I). The incident electron energy range is 50–200 eV, while the scattered electron angular range for the differential measurements is 15°–150°. In all cases the absolute scale of the differential cross sections was set using the relative flow method with helium as the reference species. Substitution effects on these cross sections, as we progress along the halomethane series CH₃F, CH₃Cl, CH₃Br, and CH₃I, are investigated as a part of this study. In addition, atomic-like behavior in these scattering systems is also considered by comparing these halomethane elastic cross sections to results from other workers for the corresponding noble gases Ne, Ar, Kr, and Xe, respectively. Finally we report results for calculations of elastic differential and integral cross sections for electrons scattering from each of the CH₃X species, within an optical potential method and assuming a screened corrected independent atom representation. The level of agreement between these calculations and our measurements was found to be quite remarkable in each case. © 2010 American Institute of Physics. [doi:10.1063/1.3319761]

I. INTRODUCTION

Methyl fluoride (CH₃F), methyl chloride (CH₃Cl), methyl bromide (CH₃Br), and methyl iodide (CH₃I) are all halomethane molecules in which one of the hydrogen atoms is replaced with the relevant halogen atom. The members of this series of molecules all play a potential role in the depletion of the Earth's protective ozone layer and all are active greenhouse gases (Ref. 1 and references therein). In addition they are also important in the chemical industry, for example, in semiconductor etching,^{1,2} as refrigerants, and as methylating agents.

It is thus not surprising that considerable work has been performed on the optical absorption (IR and VUV) spectra of these compounds.^{3–6} However, from an electron scattering perspective, the available cross section data are more limited and appears to be mainly restricted to the lighter molecules (CH₃F and CH₃Cl) in the series. In particular we highlight the grand total cross section experiments on CH₃F and CH₃Cl by Krzysztofowicz and Szmytkowski,⁷ on CH₃Br by Krzysztofowicz and Szmytkowski⁸ and on CH₃I by Szmytkowski and Krzysztofowicz,⁹ the ionization and fragmentation work in CH₃F from Moxom *et al.*¹⁰ and the detailed elastic differential and integral cross section (ICS) experiments and calculations, again for CH₃F, by Varella

*et al.*¹¹ We note that this latter work was restricted to energies in the range 1.5–30 eV, so that the present study represents an extension of that original investigation to higher incident electron energies. Having said that, we further note a 100 eV result with CH₃F from Tanaka *et al.*¹² However, as those data were not tabulated we include them here for completeness (see later). The present study also represents an original experimental contribution for elastic differential cross section (DCS) data for CH₃Cl, CH₃Br, and CH₃I. Further relevant, but low energy, elastic scattering calculations by Rescigno *et al.*¹³ (0.5–10 eV) on CH₃Cl and Natalense *et al.*¹⁴ (8–30 eV) on CH₃F and CH₃Cl are noted for completeness.

In Table I we summarize some of the important physicochemical information for each of the CH₃X (X=F, Cl, Br, and I) molecules. It is clear from this table that all the halomethanes possess strong permanent dipole moments, and also dipole polarizabilities of considerable magnitude which increase as you go from the lighter to the heavier molecules in the series. We therefore anticipate that three main factors will determine the angular and energy dependent behavior of the intermediate-energy electron-scattering cross sections: (i) halogenation effects, (ii) dipole moment magnitudes, and (iii) polarization effects. Certainly some evidence, albeit at lower energies, in support of the role of polarization effects

TABLE I. A summary of some of the important physicochemical properties of the halomethanes CH₃F, CH₃Cl, CH₃Br, and CH₃I. Also included are the dipole polarizabilities of the respective noble gases Ne, Ar, Kr, and Xe.

Species	Property ^a		Species	Property ^b
	Dipole moment (D)	Dipole polarizability (10 ⁻²⁴ cm ³)		Dipole polarizability (10 ⁻²⁴ cm ³)
CH ₃ F	1.858	2.97	Ne	0.396
CH ₃ Cl	1.892	5.35, 4.72	Ar	1.641
CH ₃ Br	1.822	5.87, 6.03, 5.55	Kr	2.484
CH ₃ I	1.620	7.97	Xe	4.044

^aCRC Handbook of Chemistry and Physics, edited by D. R. Lide, 81st edition (CRC, New York, 2000–2001).

^bCRC Handbook of Chemistry and Physics, 69th edition (CRC, New York, 1988–1989).

is provided by the complex Kohn calculations of Rescigno *et al.*¹³ It is therefore one of the purposes of this paper to investigate which, if any, of factors (i)–(iii) do actually play a significant role in the scattering description.

At intermediate energies (~50–500 eV) optical potential calculations, assuming an independent atom configuration, have proven to be a simple yet powerful tool^{15–17} in successfully predicting scattering cross sections, with application to different sized molecules. This includes smaller molecules such as water¹⁸ and tetrahydrofuran¹⁹ and, when screening corrections are included to emulate the molecular structure, larger biomolecules such as the DNA and RNA bases.²⁰ We therefore applied this approach here in order to test its applicability to the halomethane series in question. We note that in most cases this represents the first such theoretical data to become available in the literature, for those scattering systems in the energy range studied.

To first order, a bonded F-atom might exhibit some Ne-like properties, a bonded Cl-atom some Ar-like properties, a bonded Br-atom some Kr-like properties and finally a bonded I-atom some Xe-like properties. To test this, possibly naive, notion we also compare, at each energy, our elastic CH₃F DCSs with corresponding elastic DCS for Ne from Register and Trajmar,²¹ our CH₃Cl DCSs with those for Ar from Srivastava *et al.*,²² our elastic DCSs for CH₃Br with the elastic DCS of Kr from Cho *et al.*,²³ and the present elastic DCSs for CH₃I with the Xe elastic DCSs of Cho *et al.*²⁴ In this case we believe that if there is a qualitative correspondence in the DCSs, at each energy and for each species, then this might be indicative for “atomic-like” effects being important in the scattering process. In particular it would confirm that the charge distribution of the electrons in the target plays an important role in the kinematic range being considered here. Put another way, it would also indicate that the short-range static potential plays a significant role in the scattering dynamics. Note that in Table I we also include the dipole polarizabilities of the noble gases, so that a comparison to those for the halomethanes can be easily made.

In the next section of this paper we provide details of our experimental apparatus and measurement techniques. In Sec. III a brief outline of our calculations is presented, with our results and a discussion of those results coming in Sec. IV. Finally some conclusions that we have drawn from this study are given.

II. EXPERIMENTAL DETAILS

As the present data are the first taken with a new electron spectrometer recently developed at Sophia University, we describe this device in a little more detail than would usually be the case. The new spectrometer is configured in a classic crossed-beam geometry²⁵ and consists of an electron gun with hemispherical monochromator, an effusive molecular beam source (single capillary of length 6.5 mm and inner diameter 0.5 mm), and a rotatable scattered electron detector (angular range=−10° to 150°) with a second hemispherical analyzer system and a channel electron multiplier detector. Both the electron source and electron analyzer contain a number of aperture-type electron optic elements, which transport and focus the incident and scattered electrons. We note that the performance of these elements has been rigorously checked by electron trajectory calculations using the commercially available charged particle optics code from the Manchester University (UK) group. Unlike some previous apparatus at Sophia University, the present incorporates differential pumping of both the electron monochromator and the interaction region. This should reduce the effect of background gases and improve our system stability when reactive gases are being studied. Typically, a base pressure of ~1 × 10⁻⁷ torr is achieved in the main chamber when there is no gas load. In addition the spectrometer and molecular beam source are heated to a temperature of about 50 °C, in order to reduce any possible contamination during the measurements.

The overall energy resolution employed in the present experiments, at incident electron beam currents of a few nanoampere (as measured with a Faraday cup), was of the order of 120 meV [full width at half maximum (FWHM)]. Such a value means that in principle there could be contributions to the elastic signal from some of the lower-lying vibrational modes of the halomethane molecules. However, in the kinematic range of the present investigation (50–200 eV) these possible vibrational contributions are expected to be very small and can thus be ignored. The angular resolution of the new electron analyzer is ~1.5° (FWHM).

The absolute scale of the present elastic DCSs was set using the so-called relative flow technique,²⁶ in which the ratio of the elastic scattering intensity for each halomethane CH₃X to that of helium (He), under the same experimental conditions, was determined. Then employing the known helium elastic DCSs, as tabulated in Boesten and Tanaka,²⁷ we

can derive the halomethane DCSs of interest. We estimate that the experimental uncertainties on these halomethane DCSs lie in the range of 15%–20%, with the actual value depending on the specific incident electron energy (E_0) and scattered electron angle (θ_{sc}) under consideration. This overall error is largely comprised of an uncertainty in the reference He DCSs, an uncertainty in maintaining the correct flow conditions for the relative flow technique, and a much smaller error associated with the statistical accuracy of the data and the stability of the incident electron beam (<1%).

Elastic integral and momentum transfer cross sections are subsequently determined by integration of the halomethane DCSs, at each E_0 and for each species, using the well-known formulae.²⁸ The DCSs for $\theta_{sc} < 15^\circ$ and $\theta_{sc} > 150^\circ$ are obtained by an extrapolation based on our current independent atom model (IAM)-screen corrected additivity rule (SCAR) results. Nonetheless, due to the uncertainty involved in this extrapolation process, we conservatively estimate an error of ~30% on the present elastic ICSs and momentum transfer cross sections (MTCSs).

III. CALCULATIONS

The first subjects of the present calculations are the atoms constituting the molecules in question, namely, C, H, F, Cl, Br, and I. We represent each atomic target by an interacting complex potential (the so-called optical potential), whose real part accounts for the elastic scattering of the incident electrons while the imaginary part represents the inelastic processes which are considered as “absorption” from the incident beam. To construct this complex potential for each atom, we followed the procedure proposed by Staszewska *et al.*^{29,30} where the real part of the potential is represented by the sum of three terms: (i) a static term derived from a Hartree–Fock calculation of the atomic charge density distribution, (ii) an exchange term to account for the indistinguishability of the incident and target electrons, and (iii) a polarization term for the long-range interactions which depends on the target polarizability (α). The imaginary part then treats inelastic scattering as electron–electron collisions. However, we initially found some important discrepancies with the available experimental atomic scattering data, which were subsequently corrected when a correct formulation of the absorption potential³¹ was introduced. Further improvements to the original formulation,^{29,30} such as the inclusion of screening effects and in the description of the electron’s indistinguishability,¹⁵ finally led to a model which provides a good approximation for electron–atom scattering over a very broad energy range ($\sim < 1$ eV–10,000 eV).

To calculate the cross sections for electron scattering from molecules, we follow the IAM by applying what is commonly known as the additivity rule (AR). In this approach the molecular scattering amplitude is derived from the sum of all the relevant atomic amplitudes, including the phase coefficients, therefore leading to the molecular DCSs for the molecule in question. ICSs can then be determined by integrating those DCSs. Alternatively, ICSs can also be derived from the relevant atomic ICSs in conjunction with the optical theorem.¹⁵ Unfortunately, in its original form, we

TABLE II. Differential (10^{-16} cm²/sr), integral (10^{-16} cm²), and momentum transfer (10^{-16} cm²) cross sections for elastic electron scattering from CH₃F. Errors on the DCS are typically ~15%–20%, on the ICS ~30% and on the MTCS ~30%.

Angle (deg)	Energy (eV)		
	60	100	200
15	7.2117	2.5456	3.5112
20	4.0624	1.0977	1.5024
30	0.9253	0.2859	0.5534
40	0.4905	0.2521	0.2706
50	0.3519	0.2197	0.1630
60	0.2501	0.1489	0.0831
70	0.1414	0.0878	0.0631
80	0.1150	0.0629	0.0544
90	0.0744	0.0505	0.0498
100	0.0663	0.0552	0.0445
110	0.0799	0.0731	0.0412
120	0.1354	0.1071	0.0443
130	0.1906	0.1114	0.0442
140	0.0483
150	0.0566
ICS	6.123	2.929	3.253
MTCS	2.631	1.558	0.822

found an inherent contradiction between the ICSs derived from these two approaches which suggested the optical theorem was being violated.³² We, however, solved this problem by employing a normalization procedure during the computation of the DCSs, so that ICSs derived from the two approaches are now entirely consistent.³² A limitation with the AR is that no molecular structure is considered, so that it is really only applicable when the incident electrons are so fast that they effectively only see the target molecule as a sum of the individual atoms (typically when above about 100 eV). To reduce the effect of that limitation we introduced a method called SCAR,^{16,17,33} which considers the geometry of the relevant molecule (atomic positions and bond lengths) by employing some screening coefficients. With this correction the range of validity can be extended to incident electron energies as low as 20 eV. Furthermore, for polar molecules, as we are dealing with here, additional dipole–excitation cross sections can be calculated so that the range of validity of our approach may extend to energies even below 10 eV.³⁴ In the present application all the model improvements described above have been implemented in our DCS and ICS computations, for all species at each energy considered. We note, however, that the present calculations revealed that contributions from the dipole moment, for each of these molecules, are only significant for scattered electron angles below 10°, which were not experimentally accessed here. For that reason the results from those calculations were not included in the present theoretical values.

IV. RESULTS AND DISCUSSION

In Tables II–V and Figs. 1 and 2 we present our absolute elastic DCS measurements for electron scattering from the CH₃X (X=F, Cl, Br, I) halomethanes. Also included in Fig. 2 are our corresponding theoretical results from the applica-

TABLE III. Differential (10^{-16} cm²/sr), integral (10^{-16} cm²), and momentum transfer (10^{-16} cm²) cross sections for elastic electron scattering from CH₃Cl. Errors on the DCS are typically $\sim 15\%$ – 20% , on the ICS $\sim 30\%$ and on the MTCS $\sim 30\%$.

Angle (deg)	Energy (eV)		
	50	100	200
15	25.5367	6.4068	4.1544
20	12.4881	2.7054	2.6931
30	3.3058	0.8871	1.0624
40	1.3249	0.4816	0.5520
50	0.7650	0.2995	0.2430
60	0.4386	0.1671	0.2105
70	0.2781	0.1457	0.1561
80	0.2872	0.1470	0.1159
90	0.4339	0.1237	0.0897
100	0.5161	0.1080	0.0548
110	0.5295	0.0660	0.0395
120	0.4139	0.0476	0.0525
130	0.3397	0.0761	0.0861
140	0.4187	0.1433	0.1449
150	0.4569	0.2241	0.1984
ICS	14.178	6.343	5.360
MTCS	6.675	2.199	1.770

tion of our IAM-SCAR model. At the base of each of Tables II–V our elastic ICSs and MTCSs are also given, with the elastic ICS data and theory being plotted in Fig. 4.

It is clear from Figs. 1 and 2 that all the measured DCSs, at each energy studied, are very strongly peaked in magnitude at the more forward scattering angles. This result is entirely consistent with the physicochemical information we provided in Table I, namely, that all the halomethanes have strong permanent dipole moments and dipole polarizabilities of significant magnitude. However methane (CH₄), which

TABLE IV. Differential (10^{-16} cm²/sr), integral (10^{-16} cm²), and momentum transfer (10^{-16} cm²) cross sections for elastic electron scattering from CH₃Br. Errors on the DCS are typically $\sim 15\%$ – 20% , on the ICS $\sim 30\%$ and on the MTCS $\sim 30\%$.

Angle (deg)	Energy (eV)		
	50	100	200
15	10.6708	11.2205	4.1832
20	6.2053	3.6016	1.8678
30	1.7053	0.9347	0.7400
40	0.7164	0.3109	0.3165
50	0.3619	0.2547	0.2564
60	0.3292	0.2735	0.1841
70	0.3034	0.2307	0.0890
80	0.2065	0.1368	0.0413
90	0.1458	0.0697	0.0547
100	0.0974	0.0789	0.1053
110	0.0885	0.1253	0.1479
120	0.0680	0.1463	0.1179
130	0.0828	0.1096	0.0655
140	0.1118	0.0772	0.0362
150	0.1611	0.0374	0.0689
ICS	12.714	6.592	4.910
MTCS	2.220	1.704	1.436

TABLE V. Differential (10^{-16} cm²/sr), integral (10^{-16} cm²), and momentum transfer (10^{-16} cm²) cross sections for elastic electron scattering from CH₃I. Errors on the DCS are typically $\sim 15\%$ – 20% , on the ICS $\sim 30\%$ and on the MTCS $\sim 30\%$.

Angle (deg)	Energy (eV)		
	50	100	200
15	6.7517	...	5.4011
20	4.4215	2.3138	2.6824
30	0.9222	0.7218	1.2549
40	0.3883	0.7183	0.6999
50	0.2450	0.4956	0.2517
60	0.1945	0.1513	0.0871
70	0.1343	0.0988	0.2397
80	0.0655	0.1993	0.3058
90	0.0581	0.2575	0.2240
100	0.1279	0.1876	0.0756
110	0.2471	0.1213	0.0426
120	0.2922	0.1245	0.1175
130	0.2210	0.1207	0.1553
140	0.1441	0.0776	0.0993
150	0.1232	0.1326	0.0377
ICS	7.739	6.881	7.504
MTCS	2.989	2.612	1.871

has no permanent dipole moment and a relatively small dipole polarizability, also has (at 100 eV) a similar degree of forward peaking¹² in the measured DCS. This suggests that at these higher energies it might actually be direct scattering from the short-range static potential that plays the dominant role in the interaction. Interestingly, the halogenation effects on the measured DCSs, as one progressively substitutes X = F with Cl, Br, and I in CH₃X, are not so obvious for scattered electron angles less than about 30° irrespective of the incident electron energy. However, for scattering angles greater than $\sim 30^\circ$ (see Fig. 1), the effect of substituting different halogens on the methyl group causes significant changes in the angular distributions, with important structure being apparent in some cases but not in others. We also note that the halogenation effect manifests in both our measure-

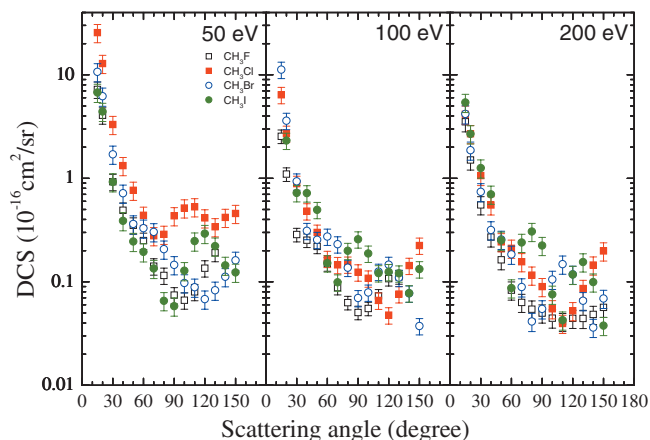


FIG. 1. Comparison of the present experimental DCSs (10^{-16} cm²/sr) for elastic electron scattering from CH₃F, CH₃Cl, CH₃Br, and CH₃I at 50, 100, and 200 eV incident electron energy. Note that for CH₃F the lowest energy was in fact 60 eV.

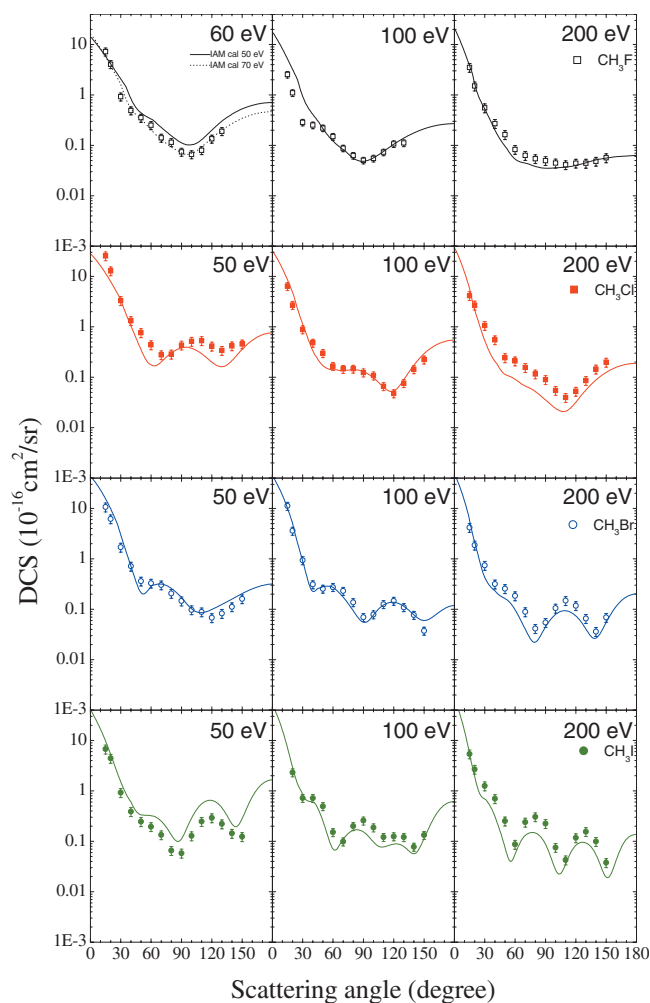


FIG. 2. Present experimental DCSs (10^{-16} cm²/sr) and corresponding calculation results for elastic electron scattering from the series of molecules CH₃X (X=F, Cl, Br and I).

ments and theory for the elastic ICSSs, as can be seen in Fig. 4. These results were not entirely unexpected as Tanaka *et al.*¹² found a conspicuous fluorination effect in their study on elastic electron scattering from the CH_{4-y}F_y ($y=0,1,2,3,4$) series of molecules, as the less electronegative H-atoms were replaced by the more electronegative F-atoms.

In Fig. 2 we compare in detail the present experimental and theoretical DCSs for each of CH₃F, CH₃Cl, CH₃Br, and CH₃I and at 50, 100, and 200 eV. From a qualitative perspective, there is excellent agreement in all cases between our measurements and calculations, with all the rich angular structure in these cross sections being observed in both. In many of the plots in Fig. 2 we also find very good agreement in terms of the magnitudes of the cross sections, between our measured and calculated data. This is particularly the case for CH₃F and CH₃Br, at each energy studied. Given that our IAM-SCAR theoretical approach is explicitly built upon scattering from atomic centers, the level of agreement seen in Fig. 2 is strong evidence in support of the assertion that atomic-like effects remain prevalent in what are fundamentally molecular systems. Further evidence in support of this notion can be seen in Fig. 3, where we compare at each incident electron energy the elastic DCS for CH₃F and Ne,²¹

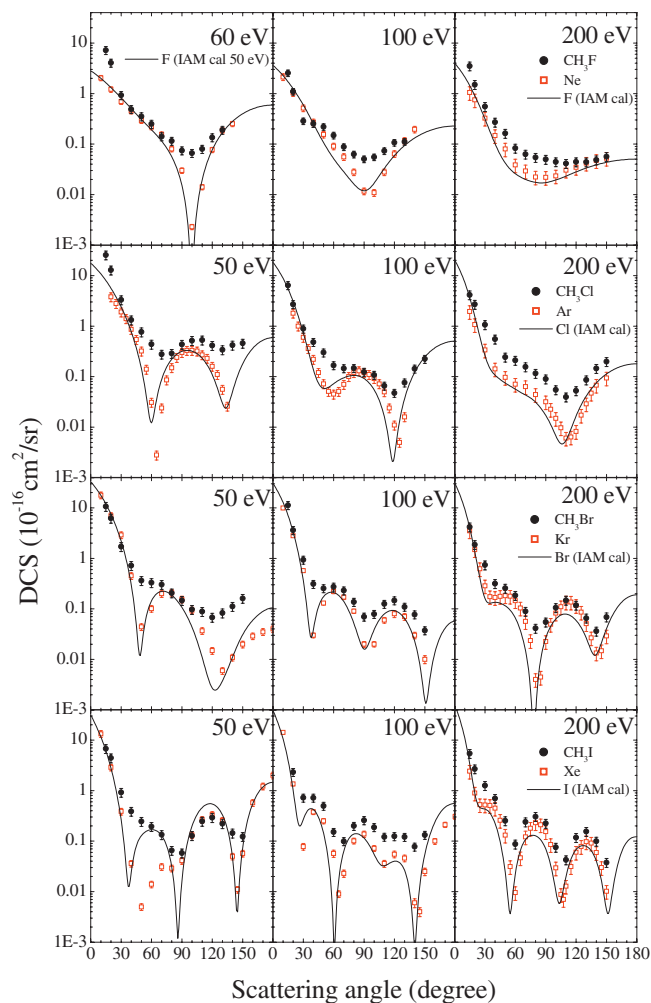


FIG. 3. A comparison between the elastic DCSs of CH₃F and Ne²¹, the elastic DCS of CH₃Cl and Ar²², the elastic DCS of CH₃Br and Kr²³, and the elastic DCSs of CH₃I and Xe²⁴ at 50, 100, and 200 eV, respectively. Note that the noble gas DCS data at 200 eV are unpublished results from Sophia University. Also included are results from our IAM-SCAR calculations for F, Cl, Br, and I.

CH₃Cl and Ar,²² CH₃Br and Kr,²³ and finally CH₃I and Xe.²⁴ In many cases the structure seen in the CH₃X halomethanes is also found, at least in part, in the corresponding noble gas species. We believe this observation suggests that a bonded F-atom behaves like Ne, a bonded Cl-atom behaves like Ar, a bonded Br-atom behaves like Kr, and a bonded I-atom behaves like Xe. In other words the bonded halogens are “acting” like their corresponding noble gas counterparts, so that atomic-like behavior manifests itself in the measured and calculated cross sections. To test this notion further, in Fig. 3 we also include results from our IAM-SCAR model for elastic scattering of electrons from the halogens F, Cl, Br, and I. Again, at each energy, the structures observed in their calculated DCSs are reminiscent of those seen in the corresponding measured CH₃X DCSs. We believe this constitutes further compelling evidence for atomic-like behavior in the scattering dynamics. Nonetheless there are differences (see Fig. 3), in particular, in regard to the magnitude of the depths of the critical minima, which suggests to us that “molecular-like” effects are still playing a role here. An alternative explanation as to why the molecular DCS are relatively

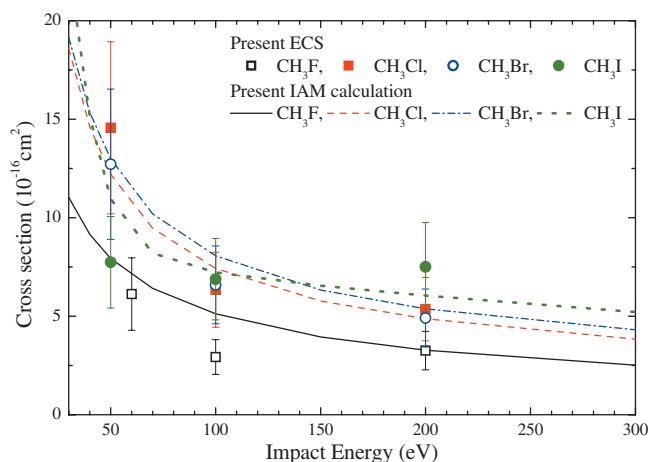


FIG. 4. Present experimental ICSs (10^{-16} cm²) and corresponding calculation results for elastic electron scattering from the series of molecules CH₃X (X=F, Cl, Br and I). Note that the acronym ECS≡elastic ICSs.

smoother was advanced by da Paixao *et al.*³⁵ In this case they argued that the observed behavior is related to the random molecular orientations in the gas. We also note that we are currently extending our measurements to lower energies, with our preliminary results suggesting that molecular-like behavior becomes increasingly important as you go to the lower incident electron energies.

Finally, in Fig. 4 we compare the present experimental and calculated ICSs for each of the species of this study. In general we find good agreement between the present experimental and theoretical ICS data although this result was to be expected, given the excellent level of agreement we had previously seen at the DCS-level (see Fig. 2). The IAM-SCAR approach has already proven its capability in providing accurate and extensive cross sections for simulations of charged-particle tracks in matter,^{18–20} in particular for biomolecules. The present study suggests it will also have good applicability for the sort of cross sections needed to model the role of electron-driven processes in low-temperature plasmas. Further work is indeed needed before this latter application could be considered to have been verified conclusively, but the results we presented here do indicate its promise in this respect.

V. CONCLUSIONS

We reported experimental elastic differential, integral, and momentum transfer cross sections for electron scattering from the halomethane molecules CH₃X (X=F, Cl, Br, and I). Corresponding theoretical differential and integral elastic cross sections from our IAM-SCAR model have also been described. Agreement between our measurements and calculations is generally very good, at each energy and for each molecule, in terms of both the absolute magnitudes of the cross sections and the shapes of the angular distributions of which many possess significant structure. This level of agreement suggests that atomic-like behavior in the scattering process survives, at least in the energy range of 50–200 eV, even though we are clearly dealing with molecular systems. Further evidence for this assertion was found when we compared the present CH₃X DCSs with elastic DCSs for Ne,

Ar, Kr, and Xe and also with IAM-SCAR results for the halogen atoms. In all cases similar structure in the angular distributions of CH₃F and Ne/F, CH₃Cl and Ar/Cl, CH₃Br and Kr/Br, and CH₃I and Xe/I, at each energy, supported our hypothesis that atomic-like behavior persists in the scattering dynamics in the kinematic range of this study. Finally, halogenation effects on the measured and calculated differential and ICSs were manifested. This is particularly true for the angular distributions for electron scattering angles greater than about 30° and was also clearly apparent in the elastic ICSs.

Perhaps the most significant result from the present work, and a result that has been observed for other complex molecular systems, is the success of the IAM-SCAR model. The mounting body of evidence which demonstrates the utility of this approach for calculating accurate cross sections for large molecular systems is impressive. The technique is relatively easy to apply and has the potential to provide the important and detailed cross section information that is required across an extensive range of energies and angles in the modeling of, for example, fields as diverse as biological radiation damage or semiconductor processing.

ACKNOWLEDGMENTS

This work was conducted under the support of the Japanese Ministry of Education, Sport, Culture and Technology and also by the Ministerio de Educación Ciencia e Innovación (Plan Nacional de Física, Project No. FIS2006-00702), the Consejo de Seguridad Nuclear and the European Science Foundation (COST Action No. CM0601). Additional support from the Australian Research Council, through its Centres of Excellence Program, and the Korea Science and Engineering Foundation (Grant No. 2009-0052415) is further noted. One of us (H.K.) also acknowledges the Japan Society for the Promotion of Science (JSPS) for his fellowships as grants-in-aid for scientific research and, most recently, to facilitate his visit to Flinders University and the ANU. Finally, we all thank Professor Yukikazu Itikawa for his important comments on this work.

- ¹N. J. Mason, *J. Phys. D* **42**, 194003 (2009).
- ²1996 Database Needs for Modeling and Simulation of Plasma Processing, National Research Council.
- ³R. Loch, B. Leyh, A. Hoxha, D. Dehareng, H. W. Jochims, and H. Baumgartel, *Chem. Phys.* **257**, 283 (2000).
- ⁴R. Loch, B. Leyh, D. Dehareng, H. W. Jochims, and H. Baumgartel, *Chem. Phys.* **317**, 87 (2005).
- ⁵S. Eden, P. Limão-Vieira, S. V. Hoffmann, and N. J. Mason, *Chem. Phys.* **331**, 232 (2007).
- ⁶T. Shimanouchi, *Tables of Molecular Vibrational Frequencies Consolidated* (NBS, Washington, 1972).
- ⁷A. M. Krzysztofowicz and C. Szymkowski, *J. Phys. B* **28**, 1593 (1995).
- ⁸A. M. Krzysztofowicz and Cz. Szymkowski, *Chem. Phys. Lett.* **219**, 86 (1994).
- ⁹Cz. Szymkowski and A. M. Krzysztofowicz, *Chem. Phys. Lett.* **209**, 474 (1993).
- ¹⁰J. Moxom, J. Xu, G. Laricchia, L. D. Hullet, D. M. Schrader, Y. Kobayashi, B. Somieski, and T. A. Lewis, *Nucl. Instrum. Methods Phys. Res. B* **143**, 112 (1998).
- ¹¹M. T. Do, N. Varela, C. Winstead, V. McKoy, M. Kitajima, and H. Tanaka, *Phys. Rev. A* **65**, 022702 (2002).
- ¹²H. Tanaka, T. Masai, M. Kimura, T. Nishimura, and Y. Itikawa, *Phys. Rev. A* **56**, R3338 (1997).

- ¹³T. N. Rescigno, A. E. Orel, and C. W. McCurdy, *Phys. Rev. A* **56**, 2855 (1997).
- ¹⁴A. P. P. Natalense, M. H. F. Bettega, L. G. Ferreira, and M. A. P. Lima, *Phys. Rev. A* **59**, 879 (1999).
- ¹⁵F. Blanco and G. García, *Phys. Rev. A* **67**, 022701 (2003).
- ¹⁶F. Blanco and G. García, *Phys. Lett. A* **317**, 458 (2003).
- ¹⁷F. Blanco and G. García, *Phys. Lett. A* **330**, 230 (2004).
- ¹⁸A. Muñoz, J. C. Oller, F. Blanco, J. D. Gorfinkiel, P. Limão-Vieira, and G. García, *Phys. Rev. A* **76**, 052707 (2007).
- ¹⁹M. Fuss, A. Muñoz, J. C. Oller, F. Blanco, D. Almeida, P. Limão-Vieira, T. P. D. Do, M. J. Brunger, and G. García, *Phys. Rev. A* **80**, 052709 (2009).
- ²⁰F. Blanco and G. García, *Phys. Lett. A* **360**, 707 (2007).
- ²¹D. F. Register and S. Trajmar, *Phys. Rev. A* **29**, 1785 (1984).
- ²²S. K. Srivastava, H. Tanaka, A. Chutjian, and S. Trajmar, *Phys. Rev. A* **23**, 2156 (1981).
- ²³H. Cho, R. P. McEachran, H. Tanaka, and S. J. Buckman, *J. Phys. B* **37**, 4639 (2004).
- ²⁴H. Cho, R. P. McEachran, S. J. Buckman, D. M. Filipović, V. Pejčev, B. P. Marinković, H. Tanaka, A. D. Stauffer, and E. C. Jung, *J. Phys. B* **39**, 3781 (2006).
- ²⁵H. Tanaka, T. Ishikawa, T. Masai, T. Sagara, L. Boesten, M. Takehawa, Y. Itikawa, and M. Kimura, *Phys. Rev. A* **57**, 1798 (1998).
- ²⁶S. K. Srivastava, A. Chutjian, and S. Trajmar, *J. Chem. Phys.* **63**, 2659 (1975).
- ²⁷L. Boesten and H. Tanaka, *At. Data Nucl. Data Tables* **52**, 25 (1992).
- ²⁸B. H. Bransden and C. J. Joachain, *Physics of Atoms and Molecules* (Longman Group, New York, 1983).
- ²⁹G. Staszewska, D. W. Schwenke, D. Thirumalai, and D. G. Truhlar, *J. Phys. B* **16**, L281 (1983).
- ³⁰G. Staszewska, D. W. Schwenke, D. Thirumalai, and D. G. Truhlar, *Phys. Rev. A* **28**, 2740 (1983).
- ³¹F. Blanco and G. García, *Phys. Lett. A* **295**, 178 (2002).
- ³²J. B. Maljković, A. R. Milosavljević, F. Blanco, D. Šević, G. García, and B. P. Marinković, *Phys. Rev. A* **79**, 052706 (2009).
- ³³F. Blanco and G. García, *J. Phys. B* **42**, 145203 (2009).
- ³⁴A. Muñoz, F. Blanco, G. Garcia, P. A. Thorn, M. J. Brunger, J. P. Sullivan, and S. J. Buckman, *Int. J. Mass Spectrom.* **277**, 175 (2008).
- ³⁵F. J. da Paixao, M. A. P. Lima, and V. McKoy, *Phys. Rev. Lett.* **68**, 1698 (1992).